RSC Advances

PAPER

Cite this: *RSC Adv.*, 2016, **6**, 106473

Zn(II) anchored onto the magnetic natural hydroxyapatite ($Zn^{II}/HAP/Fe_3O_4$): as a novel, green and recyclable catalyst for A^3-coupling reaction towards propargylamine synthesis under solvent-free conditions†

Zeinab Zarei and Batool Akhlaghinia*

Received 14th August 2016
Accepted 22nd October 2016

DOI: 10.1039/c6ra20501a

www.rsc.org/advances

In this paper, Zn(II) anchored onto the magnetic natural hydroxyapatite ($Zn^{II}/HAP/Fe_3O_4$), as a new, versatile and magnetically recoverable catalyst, was prepared and characterized using different techniques such as FT-IR, XRD, TGA, TEM, EDX, VSM and ICP. The composition of this catalyst was determined and it was clearly found that the size of the particles was about 8–30 nm and they were rod-like in shape. Also, VSM analysis showed that the synthesized nanocatalyst had superparamagnetic behavior. The new nanocatalyst has been found to effectively catalyze the synthesis of structurally different propargylamine derivatives *via* a one-pot three-component A^3-coupling reaction of terminal alkynes, aldehydes and secondary amines in high yields at 100 °C under solvent-free conditions. This green protocol provides significant advantages, such as excellent yield of products, broad substrate scope, mild reaction conditions, minimization of chemical waste, simple work-up procedure, easy preparation of catalyst and being environmentally benign. Importantly, the prepared nanocatalyst can be recovered by applying an external magnetic field and reused for seven cycles without significant loss of activity.

1. Introduction

Owing to their potent biological activities, propargylamines are an attractive class of compounds. They can act as enzyme inhibitors,[1] antitumor antibiotics,[2] herbicides,[3] and pharmaceutical agents.[4] Moreover they are versatile structural components and skeletons in natural products[4] and therapeutic drug molecules[5] and also one of the synthons for the synthesis of a variety of nitrogenous compounds such as pyrrolidines,[6a] pyrroles,[6b] pyrrolophanes,[7] aminoindolizines,[8] isoindoline,[9] imidazolidinones,[10] 2-aminoimidazoles[11] and oxazolidinones.[12] Thus, the development of new synthetic methods for propargylamines has received great attention from synthetic and medicinal chemists. In recent years, various methods have been developed for the synthesis of these compounds. Classical methods for the preparation of propargylamines are as follows: (1) direct nucleophilic attack of lithium acetylides or Grignard reagents on imines or their derivatives;[13,14] (2) direct C–C bond formation of terminal alkynes with tertiary amines *via* C–H activation;[15] (3) amination of propargylic halides, propargylic phosphates, or propargylic triflates;[16] and (4) three-component coupling of aldehydes, amines, and alkynes (A^3-coupling).[17] As multicomponent reactions (MCRs) provide an elegant means to assemble molecular complexity and diversity from simple and readily available starting materials *via* simple and efficient one-step processes,[18] the development of A^3-coupling reaction of an alkyne, aldehyde, and amine (which were utilized to construct libraries of structurally complex compounds for the evaluation of biological activities), is a continuing interest at the forefront of synthetic organic chemistry.[5a,19] However, in A^3-coupling reaction transition metal catalysts are necessary to fulfill the reaction *via* formation of metal acetylide intermediate. A number of homogeneous transition metal catalysts such as Au(I)/Au(III) salts,[20] Au(III) salen complexes,[21a] Au/CeO_2,[21b] Au NPs,[22] Cu(I) salts,[23,24] CuBr,[25] $Cu(2\text{-}EH)_2$,[26] $Cu(OTf)_2$,[27] Cu(I)/Cu(II) complex,[28] $Cu(OAc)_2$,[29] Cu(0),[30] AgI salts,[31] Fe(III) salts,[32] Zn salts,[33] Hg_2Cl_2,[34] $InCl_3$,[35a] $InBr_3$,[35b] $NiCl_2$,[36] Ir complexes,[37] Zr complex,[38] AgOAc,[39] Co(II),[40] and a Cu/Ru(II) bimetallic system[41] have been used and proven effective in A^3-coupling reactions. Additionally, to remove the difficulties in recovering these expensive catalysts from the reaction mixture which severely inhibit their wide use in industry, reusable heterogeneous metal catalysts such as LDH-$AuCl_4$,[42] Ag(I),[43a] AgTPA,[43b] Ag nanoparticles,[43c] Ag nanoparticles supported by Ni,[43d] Cu(I) complexes,[44a,44b] CuCl,[44c] silica-immobilized CuI,[44d] Ni–Y-zeolite,[45] Zn dust,[46] copper ferrite nanoparticles,[47a] nanocrystalline copper(II) oxide,[47b] copper-

---

Department of Chemistry, Faculty of Sciences, Ferdowsi University of Mashhad, 9177948974, Mashhad, Iran. E-mail: akhlaghinia@um.ac.ir; Fax: +98-51-3879-5457; Tel: +98-51-3880-5527

† Electronic supplementary information (ESI) available: General information, spectral data of organic compounds. See DOI: 10.1039/c6ra20501a

nanoparticles,[30b] Cu/C nanoparticles,[47c] impregnated copper on magnetite,[47d] copper–zeolites,[47e] Fe_3O_4 nanoparticles,[48] ferric hydrogensulfate,[49] copper(I) anchored onto MCM-41 silica,[50] Fe_3O_4@SBA-15,[51] gold nanoparticles on ZnO,[52] Cu(I) metal–organic framework,[53] CuO nanoparticles supported on graphene oxide,[54] zinc oxide,[55] Fe_3O_4–graphene oxide,[56] oxidized copper nanoparticles on titania,[57] magnesium oxide stabilized gold nanoparticles,[58] LiOTF,[59] [bmim]PF_6/CuBr,[60] nanocopper(I) oxide–zinc oxide,[61] nano magnetite supported metal ions,[62] gold nanoparticle supported on ionic liquid,[63] amberlyst A-21 supported CuI,[64] gold immobilized onto poly(ionic liquid) functionalized magnetic nanoparticles,[65] gold nanoparticles supported on polyacrylamide,[66] hydroxyapatite supported copper[44a] and nano indium oxide[67] as well as alternative energy sources like microwaves[23f,68a] and ultrasound[68b] in the presence of CuI were also developed to accomplish this three-component coupling reactions *via* C–H activation.

Nowadays, magnetic nanoparticles have attracted considerable interest due to their easy separation and also their remarkable physical and chemical properties. To avoid the aggregation of nanoparticles and to improve their chemical stability, the surface of the nanoparticles has been coated with

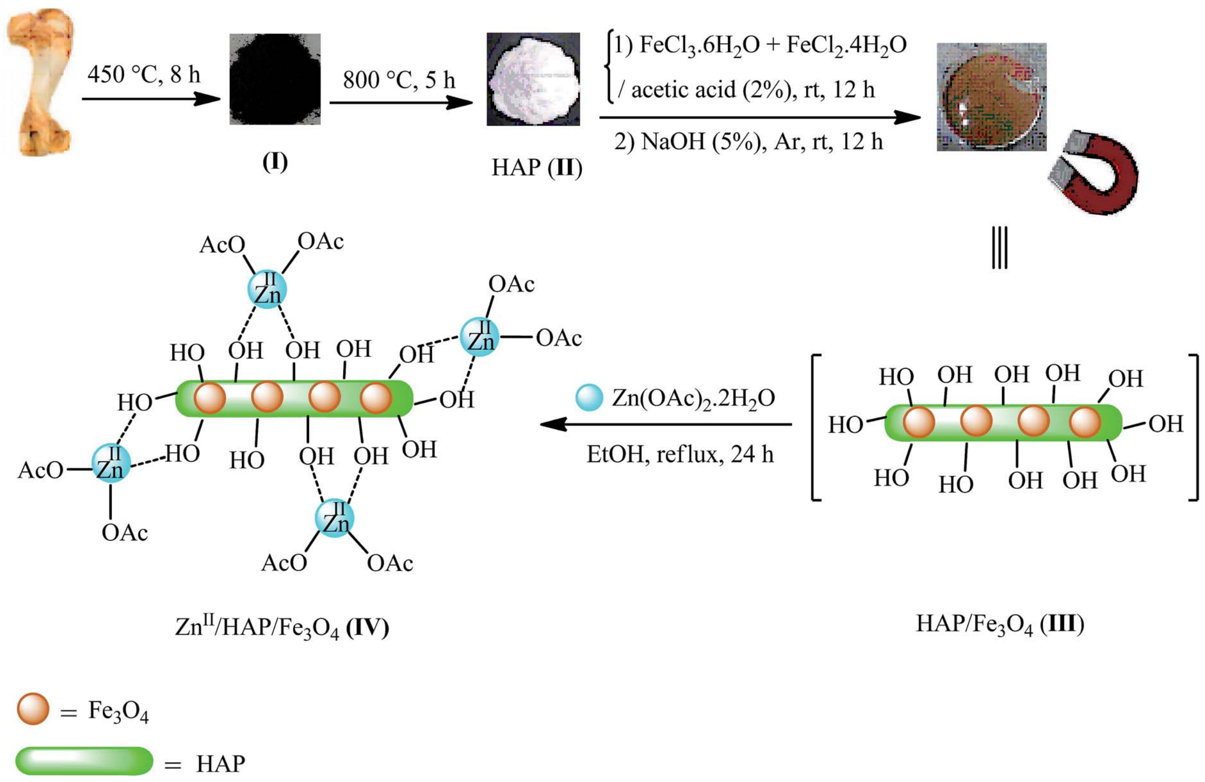

Scheme 1 Preparation of Zn(II) anchored onto the magnetic natural hydroxyapatite (Zn^{II}/HAP/Fe_3O_4).

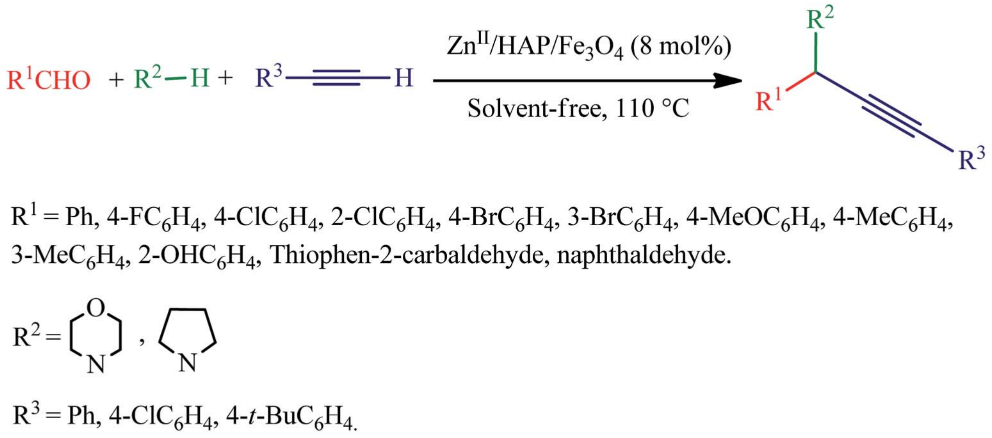

Scheme 2 Synthesis of different structurally propargylamines in the presence of Zn^{II}/HAP/Fe_3O_4 under solvent-free conditions.

different materials such as silica, zeolite, carbon, polymer and hydroxyapatite.[69] Among them hydroxyapatite (as a mineral form of calcium apatite, which is shown by $Ca_{10}(PO_4)_6(OH)_2$) is an excellent support for various heterogeneous catalysts because of the hydroxyl groups on its surface. Natural hydroxyapatite in comparison with the synthesized hydroxyapatite has several unique properties (such as lower cost of production, high specific surface area without template, safer synthetic process as well as low water solubility, availability, low cost, high stability toward oxidizing and reducing reagents and environment-friendly nature) which can make it an excellent support for the preparation of heterogeneous catalysts in organic chemistry.[70a–d] On the other hand, as the separation of hydroxyapatite from the reaction mixture is difficult, using magnetic core in the structure of hydroxyapatite is the best choice to facilitate the separation problems. Also, toxic effects of iron oxides NPs can be reduced when they are embedded into the hydroxyapatite matrix.[71] During the course of our continued interests in development of new heterogeneous catalysts[72] in organic synthesis with respect to the importance of green chemistry legislations, herein natural hydroxyapatite has been extracted from cow bones as an initial material through two burning processes to utilize the aforementioned advantages of it. Afterwards, it has been magnetized and subsequently, $Zn(OAc)_2 \cdot 2H_2O$ has been anchored on it (Scheme 1). The catalytic activity of $Zn^{II}/HAP/Fe_3O_4$ was proved for direct three-component coupling reactions of aldehydes, alkynes, and amines for the construction of propargylamines under solvent-free conditions (Scheme 2).

2. Experimental

2.1. General

All chemical reagents and solvents were purchased from Merck and Sigma-Aldrich chemical companies and were used as received without further purification. The purity determinations of the products were accomplished by TLC on silica gel polygram STL G/UV 254 plates. The FT-IR spectra were obtained using an AVATAR 370 FT-IR spectrometer (Therma Nicolet spectrometer, USA) using liquid films (neat) on NaCl plates at room temperature in the range between 4000 and 400 cm^{-1} with a resolution of 4 cm^{-1}. The NMR spectra were obtained in Bruker Avance 300 MHz instruments in $CDCl_3$. Mass spectra were recorded with a CH7A Varianmat Bremem instrument at 70 eV electron impact ionization, in *m*/*z* (rel%). Elemental analysis was performed using a Thermo Finnigan Flash EA 1112 Series instrument. TGA analysis was carried out on a Shimadzu Thermogravimetric Analyzer (TG-50) in the temperature range of 25–900 °C at a heating rate of 10 °C min^{-1} under air atmosphere. Transmission electron microscopy (TEM) was performed with a Leo 912 AB microscope (Zeiss, Germany) with an accelerating voltage of 120 kV and transmission electron microscopy (TEM) with an accelerating voltage of 150 kV was performed using TEM microscope (Philips CM30). Inductively coupled plasma (ICP) was carried out on a Varian, VISTA-PRO, CCD, Australia. Elemental compositions were determined with an SC7620 energy-dispersive X-ray analysis (EDX) presenting a 133 eV resolution at 20 kV. The magnetic property of catalyst was measured using a vibrating sample magnetometer (VSM, 7400 Lake Shore). The crystal structure of catalyst was analyzed by XRD using a D8 ADVANCE-Bruker diffractometer operated at 40 kV and 30 mA utilizing Cu Kα radiation ($\lambda = 0.154$ Å). All yields refer to isolated products after purification by thin layer chromatography.

2.2. Extraction of natural hydroxyapatite from cow bones

Natural hydroxyapatite was obtained in two-stage calcination processes from the cow bones as the raw material. In the first step, the cow bones were cleaned by washing with hot water several times to remove oily materials. In order to remove the remaining char on the bone, they were placed in an air furnace at 450 °C for 8 h which led to formation the bone ash (**I**). Then, the bone ash (**I**) was burned at 800 °C for 5 h to give a white powder that was natural hydroxyapatite (**II**).[73]

2.3. Preparation of magnetic HAP/Fe_3O_4 nanoparticles (III)

Into a 500 mL two-necked flask equipped with argon gas inlet tube, a solution of $FeCl_3 \cdot 6H_2O$ (2.1 g, 8 mmol) and $FeCl_2 \cdot 4H_2O$ (1.05 g, 5.2 mmol) in 100 mL acetic acid (2%) was added. The resulting solution was magnetically stirred for 30 min at room temperature, and then natural hydroxyapatite (**II**) (4 g) was added into the solution and vigorously stirred for 12 h to obtain a homogenous brick solution. Then the resulting mixture was quickly poured into NaOH solution (100 mL, 5%) in one portion and soaked under argon atmosphere at room temperature. After soaking for 12 h, the synthesized HAP/Fe_3O_4 nanoparticles (**III**) (as a brown powder) was collected by an external magnet, washed with distilled water (4 × 100 mL) until the pH reached 7, and then dried at ambient temperature.

2.4. Preparation of $Zn^{II}/HAP/Fe_3O_4$ nanoparticles (IV)

To a solution of $Zn(OAc)_2 \cdot 2H_2O$ (1.4 g, 6 mmol) in absolute ethanol (25 mL), the synthesized HAP/Fe_3O_4 nanoparticles (**III**) (2 g) was added and the reaction mixture was refluxed for 24 h. Subsequently, the resulting suspension was magnetically separated, washed repeatedly with water (2 × 100 mL) and dried at 60 °C for 12 h.

2.5. Typical procedure for preparation of 4-(1,3-diphenylprop-2-ynyl)morpholine (4a)

A mixture of benzaldehyde (0.1 g, 1 mmol), morpholine (0.08 g, 1 mmol), phenylacetylene (0.10 g, 1 mmol) and $Zn^{II}/HAP/Fe_3O_4$ (**IV**) (0.08 g, 8 mol%) was taken into a round-bottomed flask and stirred at 110 °C. The progress of reaction was monitored by TLC (*n*-hexane : EtOAc, 1 : 1). After completion of the reaction, the nanocatalyst was separated with an external magnet and the reaction mixture was extracted with water (2 × 10 mL) and ethyl acetate (2 × 10 mL). The organic layer was evaporated and the resulting crude product was purified by thin layer chromatography using ethyl acetate/*n*-hexane (1/1) as eluent to give the desired product. The pure 4-(1,3-diphenylprop-2-ynyl) morpholine was obtained with a 95% yield (0.25 g).

3. Results and discussion

3.1. Characterization of catalyst

Zn(II) anchored onto magnetic natural hydroxyapatite (Zn^{II}/HAP/Fe_3O_4) was synthesized according to the pathway shown in Scheme 1 as a novel, efficient and reusable heterogeneous catalyst. This newly synthesized catalyst was fully characterized by different techniques such as Fourier transform infrared spectroscopy (FT-IR), thermogravimetric analysis (TGA), transmission electron microscopy (TEM), energy-dispersive X-ray analysis (EDX), vibrating sample magnetometer (VSM), X-ray powder diffraction (XRD) and inductively coupled plasma (ICP). The results obtained from these techniques, confirmed the successful preparation of the new nanocatalyst.

The FT-IR spectra of the bone ash (**I**), HAP(II), HAP/Fe_3O_4 (**III**) and Zn^{II}/HAP/Fe_3O_4 (**IV**) were illustrated in Fig. 1a–d. As can be seen in Fig. 1a (FT-IR spectrum of **I**) the relatively broad band around 3660–3280 cm^{-1} attributed to the asymmetric and symmetric stretching vibrations of the hydroxyl groups in the bone ash matrix.[73] An absorption band at 1629 cm^{-1} was indicative of amide functional groups of the protein constituents in the organic matrix of bone ash.[74] Also, the observed band at 1471 cm^{-1} with a shoulder at 1420 cm^{-1} could be ascribed to the stretching vibration of carbonate ions.[74] Furthermore, the absorption bands appearing at 1039, 961, 605, 562 cm^{-1} were related to the stretching vibration modes of phosphate groups.[74] After heat treating of the bone ash at 800 °C, the broad band (3660–3280 cm^{-1}) was disappeared and replaced by a weak and sharp absorption band at 3571 cm^{-1} which is due to the hydroxyl stretching vibration (Fig. 1b).[74] This is in agreement with the change of color from black powder ash (**I**) to a white powder (**II**). The FT-IR spectrum of HAP/Fe_3O_4 (**III**) (Fig. 1c) showed a broad band at 3415 cm^{-1} that revealed the presence of hydroxyl groups on the surface of the magnetic nanoparticles.[75] It is worth noting that the stretching vibration bands of Fe–O bonds at around 633–565 cm^{-1} were covered by the broad stretching vibration bands of phosphate groups of hydroxyapatite which cannot be distinguished.[73] Also, the coordination of $Zn(OAc)_2 \cdot 2H_2O$ was confirmed by decreasing the intensities of absorption bands of hydroxyl groups (Fig. 1d).

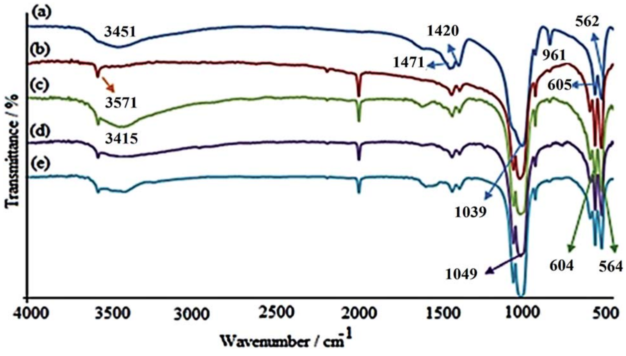

Fig. 1 FT-IR spectrum of (a) the bone ash (I), (b) HAP (II), (c) HAP/Fe_3O_4 (III), (d) Zn^{II}/HAP/Fe_3O_4 (IV) and 7th reused Zn^{II}/HAP/Fe_3O_4.

The crystal structure of the obtained HAP and Zn^{II}/HAP/Fe_3O_4 were characterized by XRD. As seen in Fig. 2a, the XRD pattern exhibited reflection peaks at around $2\Theta = 26.0°$, 32.0°, 33.1°, 34.2°, 40.0°, 46.7° and 49.5° that can be indexed to (002), (211), (300), (202), (130), (222) and (213) planes of hexagonal structure of the natural hydroxyapatite (JCPDS: 24-0033).[76,77] The strong peaks indicated phase purity of HAP nanoparticles. Moreover, in comparison with the pattern of the natural hydroxyapatite, Fig. 2b showed several additional peaks at $2\Theta = 35.4°$, 43.3°, 53.7°, 57.3° and 62.9° which assigned to the (311), (400), (422), (511) and (440) crystal planes, respectively, in Fe_3O_4 cubic lattice (JCPDS: 19-0629).[78] According to the Debye–Scherer equation, the crystallite size of Zn^{II}/HAP/Fe_3O_4 was estimated to be 30 nm. It is noteworthy that due to the use of argon atmosphere in the soaking process, no diffraction peak of Fe_2O_3 NPs was detected in the structure of the synthesized catalyst. Also, there is no obvious characteristic diffraction peaks associated to $Zn(OH)_2$ formation.[79]

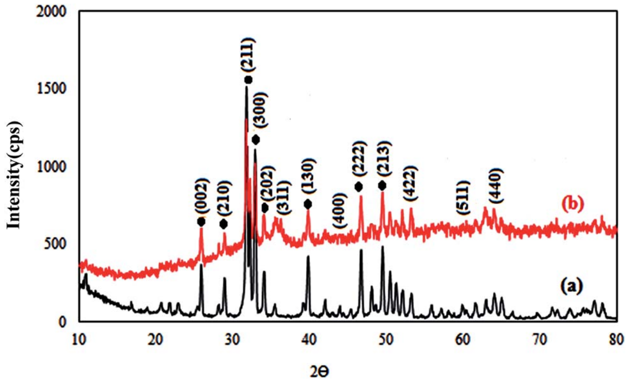

Fig. 2 The XRD patterns of (a) HAP and (b) Zn^{II}/HAP/Fe_3O_4.

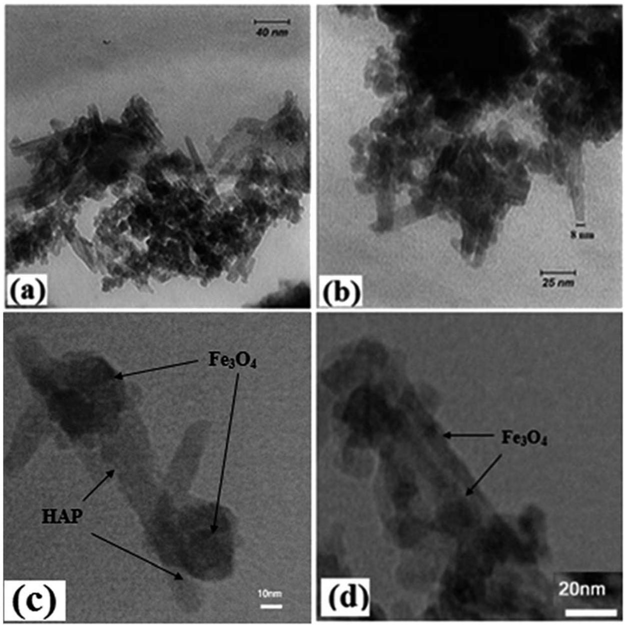

Fig. 3 TEM images with 120 kV (a and b) and 150 kV (c and d) of Zn^{II}/HAP/Fe_3O_4.

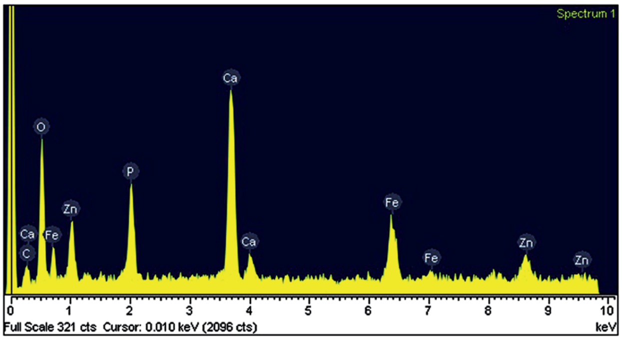

Fig. 4 The EDS analysis of $Zn^{II}/HAP/Fe_3O_4$.

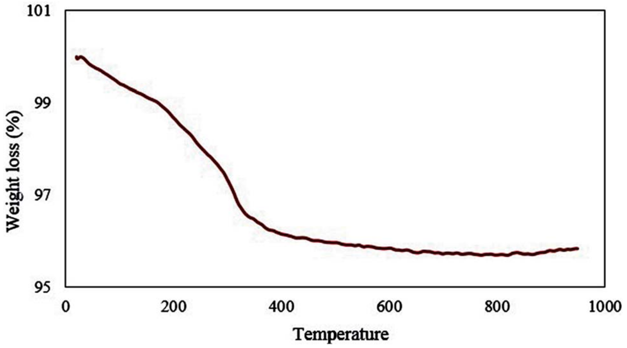

Fig. 6 TGA thermogram of $Zn^{II}/HAP/Fe_3O_4$.

Also the TEM images presented in Fig. 3a and b showed the size of particles was in the range of 8–30 nm with rod-like in shape.[80] Moreover, the images clearly show the entrapment of the Fe_3O_4 particles in the natural hydroxyapatite matrix which resulted from agglomeration of small particles and good dispersity of Fe_3O_4 NP into the HAP scaffold. Likewise, in the TEM analysis with higher voltage (150 kV), the dark particles can be distinguished from the usual brighter ones (Fig. 3c and d). Due to the stronger absorption contrast, it is clear that the dark particles are identified as iron phase (Fe_3O_4), whereas the phase containing more (brightness) pores is HAP.

Furthermore, energy dispersive spectrometer (EDS) revealed the existence of Ca, P, O, Fe and Zn elements in nanocatalyst as shown in Fig. 4. It is clear that zinc was successfully anchored onto the magnetic hydroxyapatite matrix due to the considerable intensity of Zn(II). In addition, there are no impurity elements in the nanocatalyst structure.

The magnetic behaviour of the nanocatalyst was measured using a vibrational sampling magnetometer (VSM) at room temperature. As can be seen in Fig. 5, the hysteresis loop of $Zn^{II}/HAP/Fe_3O_4$ was completely reversible which indicated a superparamagnetic behaviour. Also, the curve indicated that the saturation magnetization value of $Zn^{II}/HAP/Fe_3O_4$ was about 7.90 emu g^{-1} which was lower than the reference value for bulk Fe_3O_4 particles ($M_s = 73$ emu g^{-1}).[81] This phenomenon can be attributed to the placement of Fe_3O_4 nanoparticles into the HAP matrix. However, compared to the previously published report,[73] the magnetization value of this catalyst was almost doubled due to using argon atmosphere in the soaking process resulting in Fe_3O_4 NPs preparation method. These magnetic properties were high enough for magnetic separation of the nanocatalyst from the reaction mixture with an external magnet.

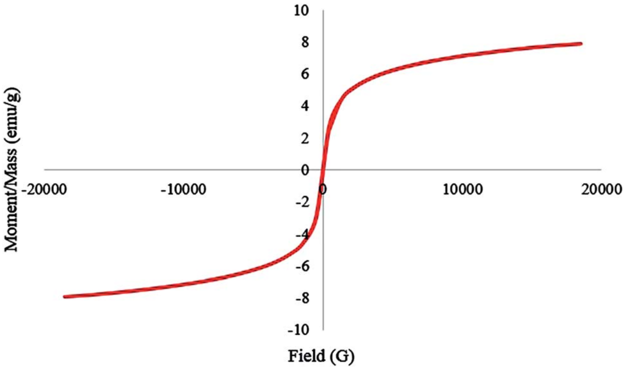

Fig. 5 Magnetization curve of $Zn^{II}/HAP/Fe_3O_4$.

Thermogravimetric analysis (TGA) of $Zn^{II}/HAP/Fe_3O_4$ was also performed to investigate the thermal stability of the catalyst. As it is obvious in Fig. 6, TGA thermogram showed three major weight-loss stages. The first stage was mainly related to the evaporation of absorbed physical and chemical water on the catalyst surface (weight loss 0.79% at 32–140 °C). The second one which was occurred at 140–450 °C (weight loss 2.99%), was corresponded to the removal of the organic segments in the structure of **III**. After that, there was a weight loss of about 0.33% ranging from 450 °C to 750 °C due to the decomposition of calcium carbonate to calcium oxide which verified the presence of natural hydroxyapatite.[74]

Besides, the total zinc content in the freshly prepared catalyst which was determined by ICP analysis is calculated to be 66 957 ppm, 0.06 g or 1.02 mmol of Zn(II) per 1.00 g of nanocatalyst.

3.2. Catalytic synthesis of propargylamines

To develop an improved catalytic system for the synthesis of propargylamines, a series of experiments were carried out by A^3-coupling reaction between benzaldehyde, morpholine and phenylacetylene and the results are summarized in Table 1. Low yield of product was produced in the absence of any catalyst as the same as in the presence of Fe_3O_4 NPs, HAP (**II**) and HAP/Fe_3O_4 (**III**), while $Zn^{II}/HAP/Fe_3O_4$ nanoparticles afforded excellent yield (Table 1, entries 1–5). In solvent-free condition, $Zn^{II}/HAP/Fe_3O_4$ nanoparticles catalyzed A^3-coupling reaction as well as in toluene (compare entry 6 with entry 5). Having found the most effective catalyst ($Zn^{II}/HAP/Fe_3O_4$ nanoparticles in solvent-free condition at 110 °C in terms of yield, cost effectiveness and reaction time), we address next optimization in terms of catalyst loading, temperature, solvent screening and molar ratio of benzaldehyde/phenylacetylene/morpholine (Table 1, entries 7–17). In the optimal process, 8 mol% of $Zn^{II}/HAP/Fe_3O_4$ nanoparticles (in solvent-free condition at 110 °C and by applying 1/1/1 molar ratio of benzaldehyde/phenylacetylene/morpholine)

Table 1 Optimization of various reaction parameters for the synthesis of 4-(1,3-diphenylprop-2-ynyl)morpholine in the presence of Zn^{II}/HAP/Fe_3O_4

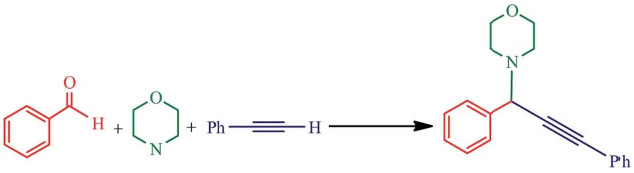

Entry	Molar ratio of (benzaldehyde/phenylacetylene/morpholine)	Catalyst (mol%)	Solvent	Temperature (°C)	Time (h)	Isolated yield (%)
1	1/1.1/1	—	Toluene	110	4/24	10/10
2[a]	1/1.1/1	0.05 (g)	Toluene	110	4/24	10/10
3[b]	1/1.1/1	0.05 (g)	Toluene	110	4/24	10/10
4[c]	1/1.1/1	0.05 (g)	Toluene	110	4/24	10/10
5	1/1.1/1	5	Toluene	110	4	95
6	1/1.1/1	5	—	110	4	95
7	1/1.1/1	6	—	110	3	80
8	1/1.1/1	7	—	110	3	85
9	1/1.1/1	8	—	110	3	95
10	1/1.1/1	9	—	110	3	95
11	1/1.1/1	10	—	110	3	95
12	1/1.1/1	8	—	100	3	80
13	1/1.1/1	8	H_2O	Reflux	3	10
14	1/1.1/1	8	PEG	110	3	30
15	1/1.1/1	8	DCM	Reflux	3	5
14	1/1.1/1	8	THF	Reflux	3	5
15	1/1.1/1	8	1,4-Dioxane	Reflux	3	0
16	1/1.1/1	8	CH_3CN	Reflux	3	20
17	1/1/1	8	—	110	3	95
18[d]	1/1/1	8	—	110	7	95

[a] The reaction was performed in the presence of Fe_3O_4 NP. [b] The reaction was performed in the presence of HAP (**II**). [c] The reaction was performed in the presence of HAP/Fe_3O_4 (**III**). [d] The reaction was performed in the presence of $Zn(OAc)_2 \cdot 2H_2O$.

generated the desired A^3-product in 95% isolated yield (Table 1, entry 17). Lower catalyst loading (below 8 mol%) resulted lower conversion while additional amounts of catalyst (9 mol% and 10 mol%) have not any considerable effects on the reaction yield and reaction rate. In the presence of the optimized amount of $Zn(OAc)_2 \cdot 2H_2O$ (8 mol% Zn(II)), the A^3-coupling reaction of benzaldehyde, morpholine and phenylacetylene is completed after 7 h (Table 1, entry 18). Therefore, we may conclude that Zn(II) anchored onto the surface of HAP/Fe_3O_4 increases the catalytic activity as well as providing easy separation of catalyst from the reaction mixture by an external magnet.

On the basis of the optimized reaction conditions in hand (Table 1, entry 17), the scope and generality of the A^3-coupling reaction were investigated by employing a variety of terminal alkynes, secondary amines and aldehydes with a wide range of functional groups to find the effectiveness of the Zn^{II}/HAP/Fe_3O_4 nanocatalyst. The results are summarized in Table 2. As depicted in Table 2, when phenylacetylene, morpholine and benzaldehyde were used as the starting substrates, the desired propargylamine was formed with an excellent yield (Table 2, entry 1), whereas the benzaldehydes bearing electron-withdrawing groups (such as fluoro, chloro and bromo) afforded the desired products **4b–4f** in 80–90% isolated yields in longer reaction times (Table 2, entries 2–6). On the other hand, benzaldehydes bearing electron-donating groups (such as methyl, hydroxyl and methoxy) afforded the corresponding products in good to excellent yields in shorter reaction times (Table 2, entries 7–10). These results can be attributed to the stability of corresponding iminium ion which markedly affect on the reaction rate (see Scheme 3). Also, 1-naphthaldehyde underwent A^3-coupling reaction with moderate rate (Table 2, entry 11). By using heteroaromatic aldehydes such as thiophene-2-carboxaldehyde, the reaction led to formation of the corresponding propargylamine in 80% isolated yield even after a long period of time (Table 2, entry 12). In addition, electronic effects on phenylacetylene were investigated and it was seen that phenylacetylenes bearing electron-rich groups/or electron-deficient groups produced the desired propargylamines in good/or moderate yields, which was probably due to the nucleophilicity power of the acetylide anion (see Scheme 3 and Table 2, entries 13–14 and 23–24). Interestingly, in all cases, when pyrrolidine was applied as a secondary amine under the identical conditions, the products were obtained in lower yields or in longer reaction times (Table 2, entries 15–24), which may be attributed to low stability of corresponding iminium ion.[82] It is important to note that aliphatic aldehydes (such as

Table 2 Synthesis of different structurally propargylamines in the presence of $Zn^{II}/HAP/Fe_3O_4$ under solvent-free condition

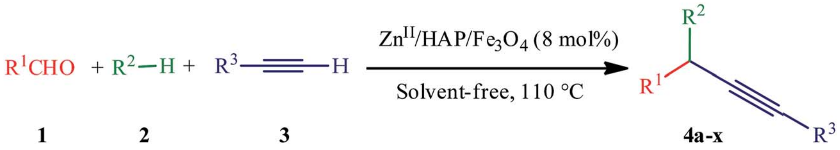

Entry	R^1	Amine (R^2)	R^3	Product	Time (h)	Isolated yield (%)
1	C_6H_5	Morpholine	C_6H_5	**4a**	3	95
2	$4\text{-}FC_6H_4$	Morpholine	C_6H_5	**4b**	7	80
3	$4\text{-}ClC_6H_4$	Morpholine	C_6H_5	**4c**	6	90
4	$2\text{-}ClC_6H_4$	Morpholine	C_6H_5	**4d**	7	90
5	$4\text{-}BrC_6H_4$	Morpholine	C_6H_5	**4e**	6	90
6	$3\text{-}BrC_6H_4$	Morpholine	C_6H_5	**4f**	6	85
7	$4\text{-}MeC_6H_4$	Morpholine	C_6H_5	**4g**	2	97
8	$3\text{-}MeC_6H_4$	Morpholine	C_6H_5	**4h**	2	95
9	$2\text{-}HOC_6H_4$	Morpholine	C_6H_5	**4i**	4	90
10	$4\text{-}MeOC_6H_4$	Morpholine	C_6H_5	**4j**	1	95
11	1-Naphthal	Morpholine	C_6H_5	**4k**	12	65
12	2-Thienyl	Morpholine	C_6H_5	**4l**	11/24	80/80
13	C_6H_5	Morpholine	$4\text{-}ClC_6H_4$	**4m**	4	70
14	C_6H_5	Morpholine	$4\text{-}t\text{-}BuC_6H_4$	**4n**	2	95
15	C_6H_5	Pyrrolidine	C_6H_5	**4o**	3	90
16	$4\text{-}FC_6H_4$	Pyrrolidine	C_6H_5	**4p**	8	60
17	$4\text{-}ClC_6H_4$	Pyrrolidine	C_6H_5	**4q**	6	80
18	$2\text{-}ClC_6H_4$	Pyrrolidine	C_6H_5	**4r**	7	80
19	$4\text{-}BrC_6H_4$	Pyrrolidine	C_6H_5	**4s**	6	85
20	$4\text{-}MeC_6H_4$	Pyrrolidine	C_6H_5	**4t**	2	95
21	$3\text{-}MeC_6H_4$	Pyrrolidine	C_6H_5	**4u**	2	90
22	$4\text{-}MeOC_6H_4$	Pyrrolidine	C_6H_5	**4v**	2.5	95
23	C_6H_5	Pyrrolidine	$4\text{-}ClC_6H_4$	**4w**	6	60
24	C_6H_5	Pyrrolidine	$4\text{-}t\text{-}BuC_6H_4$	**4x**	2.5	90

formaldehyde, cinnamaldehyde, 3-methyl butanaldehyde and 3-methyl pentaldehyde) and secondary aliphatic amines such as piperidine and piperazine did not afford the corresponding product under the same reaction conditions. These results indicate the superior properties of $Zn^{II}/HAP/Fe_3O_4$ nanocatalyst for the synthesis of structurally different propargylamines and also the selectivity of the present methodology in A^3-coupling reaction of aromatic aldehydes, morpholine and pyrrolidine.

Most of the obtained propargylamines (**4a–g**, **4i–l**, **4o–4q** and **4s–v**) were known and characterized by comparing their physical data (colour) and spectral data (mass spectrometry) with those of authentic samples reported in the literature. The structure of the selected products was further identified by FT-IR, ^{1}HNMR and ^{13}CNMR spectroscopy. The novel synthesized compounds (**4h**, **4m**, **4n**, **4r**, **4w** and **4x**) were also characterized by using elemental analysis technique. The progress of the reaction was monitored by disappearance of starting materials and formation of product on TLC which confirmed the completion of the reaction. In the FT-IR spectra of the synthesized products, disappearance of the following bands, a strong absorption band at 1703 cm^{-1} (related to the C═O stretching vibration of aldehyde), a broad band at 3334–3302 cm^{-1} (due to the N–H stretching vibration of morpholine)/or a sharp band at 3000 cm^{-1} (due to the N–H stretching vibration of pyrrolidine), a strong band at 3300 cm^{-1} (due to the ≡C–H stretching vibration), and replacing a sharp band at 2200–2100 cm^{-1} (due to the C≡C stretching vibration of terminal acetylene) by a very weak absorption band at 2230–2103 cm^{-1} (due to the C≡C stretching vibration of propargylamine), were the evidences of propargylamines formation. Also, in NMR, the methine proton and carbon (CH) were appeared at 5.34–4.69 and 60.07–49.9 ppm respectively.

Based on the reports in the literature[33b] and our experimental results, a plausible mechanism of A^3-coupling reaction catalyzed by $Zn^{II}/HAP/Fe_3O_4$ is shown in Scheme 3. At first, the terminal alkynes are coordinated to Zn(II) anchored onto HAP/Fe_3O_4 producing the alkyne complex **I**. Then, $Zn^{II}/HAP/Fe_3O_4$ inserted into the C–H bond of terminal alkynes to give the acetylide complex **II** on the surface of the nanocatalyst. In the third step, deprotonation of the acetylide complex **II** generates the zinc acetylide intermediate **III**, which interacts with the iminium ions (generated from aldehyde and secondary amine) and affords the intermediate **IV**. It is worth noting that the presence of $Zn^{II}/HAP/Fe_3O_4$ accelerates the formation of iminium salt through the coordination of the carbonyl group of aldehyde to Zn(II). Subsequently, nucleophilic attack of acetylide ion to iminium carbon results the final desired product **V**. In the following, $Zn^{II}/HAP/Fe_3O_4$ is released from the product

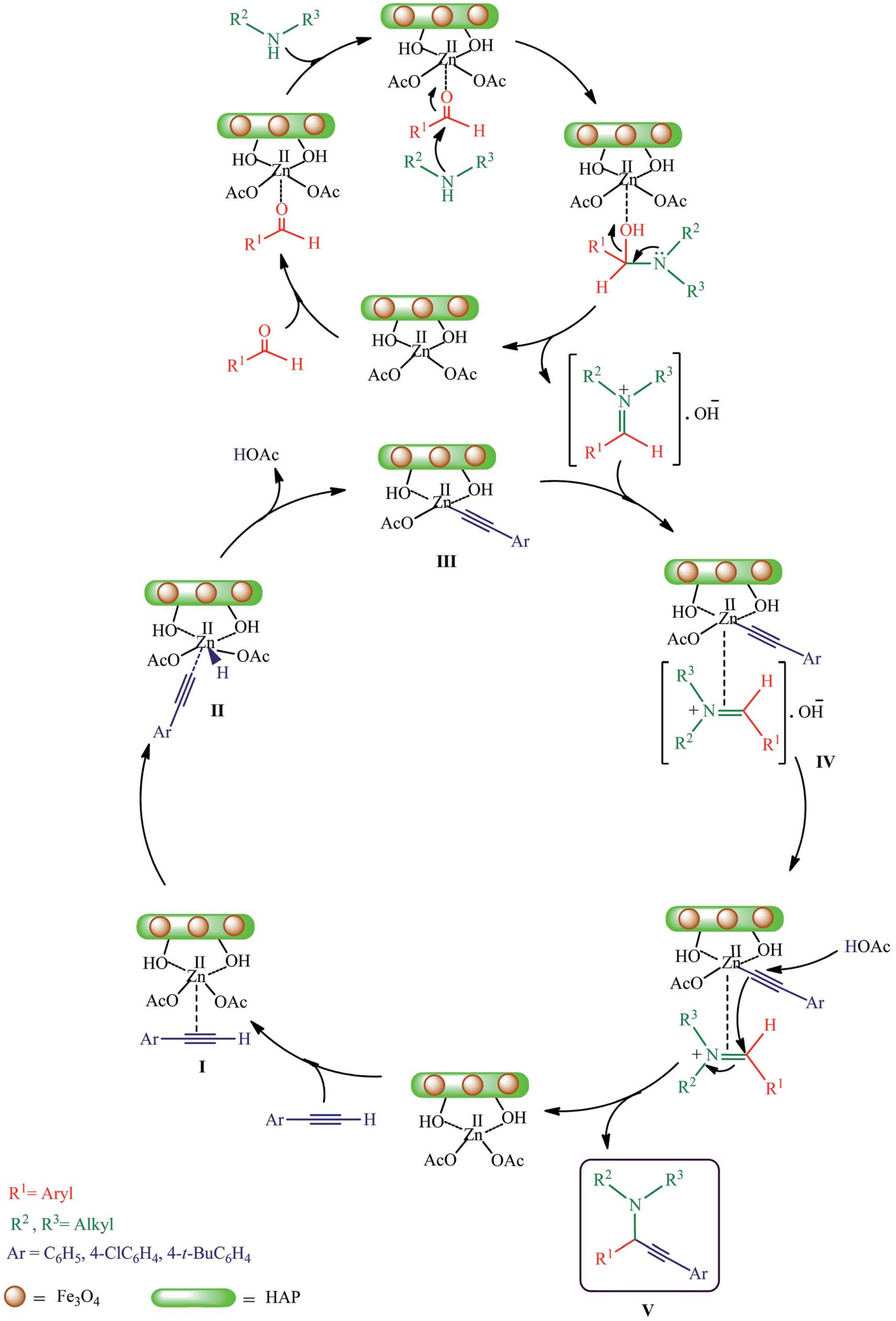

Scheme 3 Proposed reaction mechanism for the synthesis of propargylamines in the presence of Zn^{II}/HAP/Fe_3O_4.

for further cycle of reactions. With respect to the fact that aldehydes bearing electron-donating substituents react faster than aldehydes substituted with electron-withdrawing groups (because of formation more stable iminium ion, see Table 2, entries 7–10 and 20–22) it is speculated that the formation of the iminium ion can be one of the rate-determining steps of the

A^3-coupling reaction. Further studies to elucidate the mechanism are currently underway in our laboratory.

To investigate the heterogeneous nature of $Zn^{II}/HAP/Fe_3O_4$ nanocatalyst, the hot filtration test has been carried out on model reaction under the optimized condition. In this test, a mixture of $Zn^{II}/HAP/Fe_3O_4$ (0.08 g, 8 mol%), phenylacetylene (0.10 g, 1 mmol), morpholine (0.08 g, 1 mmol) and benzaldehyde (0.1 g, 1 mmol) was heated at 110 °C under solvent-free condition for 1.5 h. After 50% conversion, the catalyst was magnetically separated from the reaction mixture and then the reaction was continued for an additional time (1.5 h). No further product formation was observed which was monitored by TLC. This result clearly demonstrates that no leaching of Zn(II) took place during the reaction, and $Zn^{II}/HAP/Fe_3O_4$ is truly heterogeneous in nature.

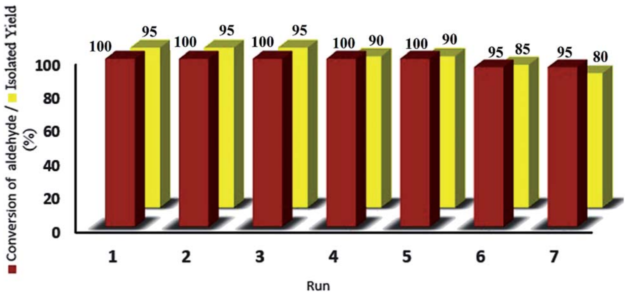

Fig. 7 Synthesis of 4-(1,3-diphenylprop-2-ynyl) morpholine in the presence of reused $Zn^{II}/HAP/Fe_3O_4$.

The reusability of the catalyst is one of the main advantages for commercial applications. Thus, to determine the reusability of the prepared nanocatalyst, after completion of the model reaction, the reaction mixture was diluted with ethyl acetate, the catalyst was magnetically separated and then washed with water (20 mL), and boiled ethyl acetate (20 mL) for several times to remove the residual of organic compounds. Then the nanocatalyst was dried at 60 °C for 12 h and used for subsequent runs under the same reaction conditions. The catalytic activity of the catalyst was remained without any noteworthy loss of activity for seven successive runs as it can be seen in Fig. 7. The excellent catalytic activity of the nanocatalyst during the recovery process have been verified by these results. Also, as can be seen in Fig. 1e, the shape of the characteristic peaks were well preserved and no significant change was occurred in the structure of the nanocatalyst after repeated cycles of the reaction. ICP analysis showed that freshly prepared catalyst contains 66 957 ppm, 0.066 g or 1.02 mmol of Zn(II) per 1 g of the catalyst, while the 7th reused catalyst contains 61 788 ppm, 0.061 g or 0.94 mmol of Zn(II) per 1 g of the catalyst. It indicates that 93% of Zn(II) could be found in the structure of the catalyst after seven runs.

To show the efficiency of $Zn^{II}/HAP/Fe_3O_4$ over some of the reported catalysts in the literature, we compared the catalytic performance of $Zn^{II}/HAP/Fe_3O_4$ in the synthesis of 4-(1,3-diphenylprop-2-yn-1-yl) morpholine with various catalysts (Table 3). As is shown in Table 3, some of these methods suffer from one or more of the following drawbacks, such as requiring

Table 3 Comparison between efficiency of $Zn^{II}/HAP/Fe_3O_4$ and some other catalysts for the synthesis of 4-(1,3-diphenylprop-2-ynyl) morpholine

Entry	Catalyst (mol%)	Molar ratio[a]	Solvent	Temp (°C)	Time (h)	Yield (%)	Ref.
1	Au/CeO_2, Au/ZrO_2 (0.10 g)	1/1.2/1.3	H_2O	100	12	83	21*b*
2	Au@GO (1)	1/1.2/1.3	H_2O	100	18	90	83
3	Fe_3O_4 NPs/GO-CuONPs (0.02 g)	1/2/3	EtOH	90	24	87	54
4	Fe_3O_4@SBA-15 (5)	1/1.2/1.5	Toluene	110	8	72	51
5	$Cu(OH)–Fe_3O_4$ (3)		Toluene	120	3	99	47*d*
6	$CuFe_2O_4$ (6.50)	1/1.2/1.3	Toluene	80	4	85	47*a*
7	Cu(I)–N_2S_2[b]-salen (3)	1/1.1/1.2	Toluene	80	4	92	50*a*
8	Cu^0–Mont (0.05)	1/1/1.2	Toluene	110	3	90	84
9	CuO (10)	1/1.3/1.5	Toluene	90	8	65	47*b*
10	$[Cu(N_2S_2)]Cl$@Y-zeolite (0.68 g)	1/1.1/1.2	DCE	70	12	90	44*b*
11	CuHAP (0.10 g)	1/1.2/1.3	CH_3CN	Reflux	6	70	44*a*
12	$NiCl_2$ (10)	1/1.2/1.5	Toluene	111	8	88	36
13	$Zn(OAc)_2 \cdot 2H_2O$ (15)	1/1.3/1.5	Toluene	Reflux	7	96	33*b*
14	CuCN (2)	1/1.2/1.5	$[bmim]PF_6$	120	2	95	24*d*
15	CuI (10)	1/1.2/1.5	PEG	100	12	92	24*b*
16	CuI (3)	1/1.2/1.5	Toluene	100	6	98	24*c*
17	$[AQ_2Cu(II)]$(5)	1/1.1/1.1	Solvent-free	100	70[c]	96	85
18	$Cu[(CH_3CN)n(PPh_3)]Br$ (5)	1//1/1	Toluene	80	85	44	28*c*
19	$CuPy_2Cl_2$ (1)	1/1.5/1.5	Solvent-free	95	40[c]	90	86
20	Cu(salen) (3)	1/1.2/1.5	Solvent-free	80	2.5	85	28*a*
21	ZnO (10)	1/1/1	Solvent-free	100	2	95	55
22	Cu_2O/ZnO (0.01 g)	1/1.2/1.5	Solvent-free	100	1	95	61
23	CuNPs/TiO_2 (0.50)	1/1/1	Solvent-free	70	7	91	57
24	$Zn^{II}/HAP/Fe_3O_4$ (8)	1/1/1	Solvent-free	110	3	95	Present study

[a] Molar ratio of (aldehyde/amine/alkyne). [b] Bis[2-(phenylthio)benzylidene]-1,2-ethylenediamine. [c] Minute.

long reaction time to achieve the reasonable yield (Table 3, entries 1–3), using toxic solvents (Table 3, entries 4–11), and homogenous catalysts (Table 3, 12–19) and moreover, a difficult process to separate heterogeneous catalysts by filtration, or centrifugation (Table 3, 20–23). Therefore, using $Zn^{II}/HAP/Fe_3O_4$ as an efficient and green nanomagnetic catalyst can remove these drawbacks; in addition, it can be easily separated from the reaction mixture by an external magnet. These results proved that our method is superior to the other previous methods in the literature.

4. Conclusion

In conclusion, aiming to contribute in innovation of green chemistry, Zn(II) anchored onto magnetic natural hydroxyapatite as a novel, versatile and magnetically recoverable nanocatalyst was synthesized and fully characterized using FT-IR, XRD, TGA, TEM, EDX, VSM and ICP techniques. Characterization results revealed that the size of particles was about 8–30 nm, rod-like in shape, and the new nanocatalyst had a strong magnetic property. Subsequently, the new nanocatalyst has been used for the synthesis of structurally different propargylamines *via* a one-pot three-component A^3-coupling reaction of terminal alkynes, aldehydes and secondary amines with high yields in green media without requiring any additives or co-catalyst. Excellent yields of products, elimination of toxic organic solvents and hazardous materials, simple work-up procedure, using inexpensive metal, simple preparation of catalyst, recovering catalyst using magnetic separation technique and being recycled at least for seven times without significant decrease in activity are the most remarkable features of this method. Also, this method can be applied for a large variety of terminal alkynes and aldehydes. Thus, this approach can be of great help for synthesizing this class of compounds for the potential applications in medicine as pharmaceutical agents and also in chemistry as synthons for the synthesis of a variety of important nitrogenous compounds without difficulties.

Acknowledgements

The authors gratefully acknowledge the partial support of this study by Ferdowsi University of Mashhad Research Council (Grant no. p/3/29781).

Notes and references

1 (*a*) C. S. Kauffman, G. D. Harris, R. L. Dorow, B. R. P. Stone, R. L. Parsons, J. A. Pesti, N. A. Magnus, J. M. Fortunak, P. N. Confalone and W. A. Nugent, *Org. Lett.*, 2000, **2**, 3119; (*b*) J. Wright, T. F. Gregory, S. R. Kesten, P. A. Boxer, K. A. Serpa, L. T. Meltzer and L. Wise, *J. Med. Chem.*, 2000, **43**, 3408; (*c*) P. H. Yu, B. A. Davis and A. A. Boulton, *J. Med. Chem.*, 1992, **35**, 3705.

2 (*a*) A. A. Boulton, B. A. Davis, D. A. Durden, L. E. Dyck, A. V. Juorio, X. M. Li, I. A. Paterson and P. H. Yu, *Drug Dev. Res.*, 1997, **42**, 156; (*b*) J. Golik, J. Clardy, G. Dubay, G. Groenewold, H. Kawaguchi, M. Koniashi, B. Krishnan, H. Ohkuma, K. Saitoh and T. W. Doyle, *J. Am. Chem. Soc.*, 1990, **112**, 3715.

3 C. Swithenbank, P. J. McNulty and K. L. Viste, *J. Agric. Food Chem.*, 1971, **19**, 417.

4 (*a*) K. Mihara, T. Aoki, A. Moriguchi, H. Yamamoto, M. Maeda, N. Tojo, T. Yamanaka, M. Ohkubo, N. Matsuoka, J. Seki and S. Mutoh, *Drug Dev. Res.*, 2004, **61**, 233; (*b*) K. Yamada and K. Tomioka, *Chem. Rev.*, 2008, **108**, 2874.

5 (*a*) Z. Jiang, P. Lu and Y. Wang, *Org. Lett.*, 2012, **14**, 6266; (*b*) S. Hase, Y. Kayaki and T. Ikariya, *Organometallics*, 2013, **32**, 5285; (*c*) Y. Yamamoto, H. Hayashi, T. Saigoku and H. Nishiyama, *J. Am. Chem. Soc.*, 2005, **127**, 10804.

6 (*a*) D. F. Harvey and D. M. Sigano, *J. Org. Chem.*, 1996, **61**, 2268; (*b*) Y. Hu, C. Wang, D. Wang, F. Wu and B. Wan, *Org. Lett.*, 2013, **15**, 3146.

7 A. Fürstner, H. Szillat and F. Stelzer, *J. Am. Chem. Soc.*, 2000, **122**, 6785.

8 B. Yan and Y. Liu, *Org. Lett.*, 2007, **9**, 4323.

9 E. R. Bonfield and C. J. Li, *Adv. Synth. Catal.*, 2008, **350**, 370.

10 O. P. Pereshivko, V. A. Peshkov, J. Jacobs, L. V. Meervelt and E. V. V. Eycken, *Adv. Synth. Catal.*, 2013, **355**, 781.

11 D. S. Ermolat'ev, J. B. Bariwal, H. P. L. Steenackers, S. C. J. De Keersmaecker and E. V. V. Eycken, *Angew. Chem., Int. Ed.*, 2010, **49**, 9465.

12 W. J. Yoo and C. J. Li, *Adv. Synth. Catal.*, 2008, **350**, 1503.

13 T. Murai, Y. Mutoh, Y. Ohta and M. Murakami, *J. Am. Chem. Soc.*, 2004, **126**, 5968.

14 (*a*) M. E. Jung and A. Huang, *Org. Lett.*, 2000, **2**, 2659; (*b*) F. Tubery, D. S. Grierson and H. P. Husson, *Tetrahedron Lett.*, 1987, **28**, 6457.

15 (*a*) M. Niu, Z. Yin, H. Fu, Y. Jiang and Y. Zhao, *J. Org. Chem.*, 2008, **73**, 3961; (*b*) Z. Li and C. J. Li, *J. Am. Chem. Soc.*, 2004, **126**, 11810; (*c*) Z. Li and C. J. Li, *Org. Lett.*, 2004, **6**, 4997.

16 (*a*) Y. Imada, M. Yuassa, I. Nakamura and S. I. Murahashi, *J. Org. Chem.*, 1994, **59**, 2282; (*b*) S. Czerneck and J. M. Valery, *J. Carbohydr. Chem.*, 1990, **9**, 767; (*c*) I. E. Kopka, Z. A. Fataftah and M. W. Rathke, *J. Org. Chem.*, 1980, **45**, 4616.

17 For reviews: (*a*) V. V. Kouznetsov and L. Y. V. Méndez, *Synthesis*, 2008, 491; (*b*) C. Wei, Z. Li and C. J. Li, *Synlett*, 2004, 1472.

18 (*a*) B. B. Toure and D. G. Hall, *Chem. Rev.*, 2009, **109**, 4439; (*b*) M. Shiri, *Chem. Rev.*, 2012, **112**, 3508; (*c*) A. K. Gupta, N. Singh and K. N. Singh, *Curr. Org. Chem.*, 2013, **17**, 474.

19 L. Zani and C. Bolm, *Chem. Commun.*, 2006, 4263.

20 (*a*) C. Wei and C.-J. Li, *J. Am. Chem. Soc.*, 2003, **125**, 9584; (*b*) H. M. Ko, K. K. Kung, J. F. Cui and M. K. Wong, *Chem. Commun.*, 2013, **49**, 8869.

21 (*a*) V. K.-Y. Lo, Y. Liu, M.-K. Wong and C.-M. Che, *Org. Lett.*, 2006, **8**, 1529; (*b*) X. Zhang and A. Corma, *Angew. Chem., Int. Ed.*, 2008, **47**, 4358.

22 D. Aguilar, M. Contel and E. P. Urriolabeitia, *Chem.–Eur. J.*, 2010, **16**, 9287.

23 (*a*) L. Shi, Y.-Q. Tu, M. Wang, F.-M. Zhang and C.-A. Fan, *Org. Lett.*, 2004, **6**, 1001; (*b*) G. W. Kabalka, L. Wang and R. M. Pagni, *Synlett*, 2001, 676; (*c*) N. Gommermann and

P. Knochel, *Chem.–Eur. J.*, 2006, **12**, 4380; (*d*) A. Bisai and V. K. Singh, *Org. Lett.*, 2006, **8**, 2405; (*e*) H. Feng, D. S. Ermolat'ev, G. Song and E. V. Eycken, *J. Org. Chem.*, 2011, **76**, 7608; (*f*) J. B. Bariwal, D. S. Ermolat'ev, T. N. Glasnov, K. V. Hecke, V. P. Mehta, L. V. Meervelt, C. O. Kappe and E. V. Eycken, *Org. Lett.*, 2010, **12**, 2774; (*g*) J. B. Bariwal, D. S. Ermolat'ev and E. V. Eycken, *Chem.–Eur. J.*, 2010, **16**, 3281; (*h*) C. Zhao and D. Seidel, *J. Am. Chem. Soc.*, 2015, **137**, 4650; (*i*) A. S. Lee, G.-A. Chen, Y.-T. Chang and S.-F. Chu, *Synlett*, 2009, 441; (*j*) Y. Kim and H. Nakamura, *Synlett*, 2012, 1686; (*k*) J. Lim, K. Park, A. Byeun and S. Lee, *Tetrahedron Lett.*, 2014, **55**, 4875.

24 (*a*) C. Wei and C.-J. Li, *J. Am. Chem. Soc.*, 2002, **124**, 5638; (*b*) Q. Zhang, J.-X. Chen, W.-X. Gao, J.-C. Ding and H.-Y. Wu, *Appl. Organomet. Chem.*, 2010, **24**, 809; (*c*) G. Ren, J. Zhang, Z. Duan, M. Cui and Y. Wu, *Aust. J. Chem.*, 2009, **62**, 75; (*d*) S. B. Park and H. Alper, *Chem. Commun.*, 2005, 1315.

25 (*a*) N. Gommermann, C. Koradin, K. Polborn and P. Knochel, *Angew. Chem., Int. Ed.*, 2003, **42**, 5763; (*b*) L. Zhou, D. S. Bohle, H.-F. Jiang and C.-J. Li, *Synlett*, 2009, 937; (*c*) K. Zhang, Y. Huang and R. Chen, *Tetrahedron Lett.*, 2010, **51**, 5463; (*d*) N. Guo and J.-X. Ji, *Tetrahedron Lett.*, 2012, **53**, 4797.

26 D. Das, A. X. Sun and D. Seidel, *Angew. Chem., Int. Ed.*, 2013, **52**, 3765.

27 (*a*) M. Ohara, Y. Hara, T. Ohnuki and S. Nakamura, *Chem.–Eur. J.*, 2014, **20**, 1; (*b*) N. Sakai, N. Uchida and T. Konakahara, *Synlett*, 2008, 1515.

28 (*a*) M. Tajbaksh, M. Farhang, H. Mardani, R. Hosseinzadeh and Y. Sarrafi, *Chin. J. Catal.*, 2013, **34**, 2217; (*b*) A. Bisai and V. Singh, *Tetrahedron*, 2012, **68**, 3480; (*c*) H. Naeimi and M. Moradian, *Tetrahedron*, 2014, **25**, 429.

29 (*a*) Z. Xu, X. Yu, X. Feng and M. Bao, *J. Org. Chem.*, 2011, **76**, 6901; (*b*) J. Wang, Q. Shen, P. Li, Y. Penga and G. Song, *Org. Biomol. Chem.*, 2014, **12**, 5597.

30 (*a*) T. Mitamura and A. Ogawa, *Org. Lett.*, 2009, **11**, 2045; (*b*) M. Kidwai, V. Bansal, N. K. Mishra, A. Kumar and S. Mozumdar, *Synlett*, 2007, 1581; (*c*) Y. Zhu, H. Zhao and Y. Wei, *Synthesis*, 2013, 952.

31 C. Wei, Z. Li and C.-J. Li, *Org. Lett.*, 2003, **5**, 4473.

32 J. Gao, Q.-W. Song, L.-N. He, Z.-Z. Yang and X.-Y. Dou, *Chem. Commun.*, 2012, **48**, 2024.

33 (*a*) L. Zani, S. Alesi, P. G. Cozzi and C. Bolm, *J. Org. Chem.*, 2006, **71**, 1558; (*b*) E. Ramu, R. Varala, N. Sreelatha and S. R. Adapa, *Tetrahedron Lett.*, 2007, **48**, 7184.

34 L. P. Hua and W. Lei, *Chin. J. Chem.*, 2005, **23**, 1076.

35 (*a*) Y. Zhang, P. Li, M. Wang and L. Wan, *J. Org. Chem.*, 2009, **74**, 4364; (*b*) J. S. Yadav, B. V. S. Reddy, A. V. H. Gopal and K. S. Patil, *Tetrahedron Lett.*, 2009, **50**, 3493.

36 S. Samai, G. C. Nandi and M. S. Singh, *Tetrahedron Lett.*, 2010, **51**, 5555.

37 (*a*) C. Fischer and E. M. Carreira, *Org. Lett.*, 2001, **3**, 4319; (*b*) S. Sakaguchi, T. Mizuta, M. Furuwan, T. Kubo and Y. Ishii, *Chem. Commun.*, 2004, 1638.

38 (*a*) L. C. Akullian, M. L. Snapper and A. H. Hoveyda, *Angew. Chem., Int. Ed.*, 2003, **42**, 4244; (*b*) J. F. Traverse, A. H. Hoveyda and M. L. Snapper, *Org. Lett.*, 2003, **5**, 3273.

39 X. Chen, T. Chen, Y. Zhou, C.-T. Au, L.-B. Han and S.-F. Yin, *Org. Biomol. Chem.*, 2014, **12**, 247.

40 W.-W. Chen, H.-P. Bi and C.-J. Li, *Synlett*, 2010, 475.

41 C. Wei, J. T. Mague and C.-J. Li, *Proc. Natl. Acad. Sci. U. S. A.*, 2004, **101**, 5749.

42 M. L. Kantam, B. V. Prakash, C. R. V. Reddy and B. Sreedhar, *Synlett*, 2005, 2329.

43 (*a*) P. Li, L. Wang, Y. Zhang and M. Wang, *Tetrahedron Lett.*, 2008, **49**, 6650; (*b*) K. M. Reddy, N. S. Babu, I. Suryanarayana, P. S. S. Prasad and N. Lingaiah, *Tetrahedron Lett.*, 2006, **47**, 7563; (*c*) W. Yan, R. Wang, Z. Xu, J. Xu, L. Lin, Z. Shen and Y. Zhou, *J. Mol. Catal. A: Chem.*, 2006, **255**, 81; (*d*) S. Wang, X. He, L. Song and Z. Wang, *Synlett*, 2009, 447.

44 (*a*) B. M. Choudary, C. Sridhar, M. L. Kantam and B. Sreedhar, *Tetrahedron Lett.*, 2004, **45**, 7319; (*b*) H. Naeimi and M. Moradian, *Appl. Catal., A*, 2013, **467**, 400; (*c*) B. Sreedhar, P. S. Reddy, C. S. V. Krishna and P. V. Babu, *Tetrahedron Lett.*, 2007, **48**, 7882; (*d*) P. R. Likhar, S. Roy, M. Roy, M. S. Subhas, M. L. Kantam and R. L. De, *Synlett*, 2007, 2301.

45 K. Namitharan and K. Pitchumani, *Eur. J. Org. Chem.*, 2010, **2010**, 411.

46 M. L. Kantam, V. Balasubrahmanyam, K. B. S. Kumar and G. T. Venkanna, *Tetrahedron Lett.*, 2007, **48**, 7332.

47 (*a*) M. L. Kantam, J. Yadav, S. Laha and S. Jha, *Synlett*, 2009, 1791; (*b*) M. L. Kantam, S. Laha, J. Yadav and S. Bhargava, *Tetrahedron Lett.*, 2008, **49**, 3083; (*c*) H. Sharghia, R. Khalifeh, F. Moeini, M. H. Beyzavi, A. Salimi Beni and M. M. Doroodmand, *J. Iran. Chem. Soc.*, 2011, **8**, 89; (*d*) M. J. Aliaga, D. J. Ramón and M. Yus, *Org. Biomol. Chem.*, 2010, **8**, 43; (*e*) M. K. Patil, M. Keller, B. M. Reddy, P. Pale and J. Sommer, *Eur. J. Org. Chem.*, 2008, **2008**, 4440.

48 (*a*) B. Sreedhar, A. S. Kumar and P. S. Reddy, *Tetrahedron Lett.*, 2010, **51**, 1891; (*b*) S. Kaur, M. Kumar and V. Bhalla, *Chem. Commun.*, 2012, **51**, 16327.

49 H. Eshghi, G. H. Zohuri and S. Damavandi, *Cent. Eur. J. Chem.*, 2011, **2**, 100.

50 (*a*) H. Naeimi and M. Moradian, *Appl. Organomet. Chem.*, 2013, **27**, 300; (*b*) F. Nadora, M. A. Volpeb, F. Alonsoc, A. Feldhoffd, A. Kirschninge and G. Radivoya, *Appl. Catal., A*, 2013, **455**, 39.

51 D. Bhuyana, M. Saikia and L. Saikia, *Catal. Commun.*, 2014, **58**, 158.

52 M. Bejar, K. Peters, M. Grenier and J. C. Scaiano, *Chem. Commun.*, 2013, **49**, 1732.

53 P. Li, S. Regati, H.-C. Huang, H. D. Arman, B.-L. Chen and J. Zhao, *Chin. Chem. Lett.*, 2014, **26**, 6.

54 M. Mirabedini, E. Motamedi and M. Zaman Kassaee, *Chin. Chem. Lett.*, 2015, **26**, 1085.

55 M. Hosseini-Sarvari and F. Moeini, *Comb. Chem. High Throughput Screening*, 2014, **17**, 439.

56 P. Mandal and A. P. Chattopadhyay, *Dalton Trans.*, 2015, 11444.

57 M. Albaladejo, F. Alonso, Y. Moglie and M. Yus, *Eur. J. Org. Chem.*, 2012, **2012**, 3093.

58 K. Layek, R. Chakravarti, M. L. Kantam, H. Maheswarana and A. Vinu, *Green Chem.*, 2011, **13**, 2878.

59 S. D. Dindulkar, B. Kwan, K. T. Lim and Y. T. Jeong, *J. Chem. Sci.*, 2013, **125**, 101.

60 J. S. Yadav, B. V. S. Reddy, V. Naveenkumar, R. S. Rao and K. Nagaiah, *New J. Chem.*, 2004, **28**, 335.

61 M. Hosseini-Sarvari and F. Moeini, *New J. Chem.*, 2014, **38**, 624.

62 M. Tajbakhsh, M. Farhang, S. M. Baghbanian, R. Hosseinzadeh and M. Tajbakhsh, *New J. Chem.*, 2014, **39**, 1827.

63 S. K. Movahed, N. F. Lehi and M. Dabiri, *RSC Adv.*, 2014, **4**, 42155.

64 G. Bosica and J. Gabarretta, *RSC Adv.*, 2015, **5**, 46074.

65 F. M. Moghaddam and A. Pourjavadi, *RSC Adv.*, 2015, **5**, 34502.

66 M. Gholinejad, F. Hamed and C. Nájera, *Synlett*, 2016, **27**, 1193.

67 M. Rahman, A. K. Majee, A. Majee and A. Hajra, *Tetrahedron Lett.*, 2011, **52**, 4437.

68 (*a*) N. E. Leadbeater, H. M. Torenius and H. Tye, *Mol. Diversity*, 2003, **7**, 135; (*b*) B. Sreedhar, P. S. Reddy, B. V. Prakash and A. Ravindra, *Tetrahedron Lett.*, 2005, **46**, 7019.

69 Y. Zhang and C. Xia, *Appl. Catal., A*, 2009, **366**, 141.

70 (*a*) Y. Masuyama, K. Yoshikawa, N. Suzuki, K. Hara and A. Fukuoka, *Tetrahedron Lett.*, 2011, **52**, 6916; (*b*) Y. Fenga, J.-L. Gonga, G.-M. Zenga, Q.-Y. Niua, H.-Y. Zhanga, C.-G. Niu, J.-H. Deng and M. Yan, *Chem. Eng. J.*, 2010, **162**, 487; (*c*) F. Zhuang, R. Tan, W. Shen, X. Zhang, W. Xu and W. Song, *J. Alloys Compd.*, 2015, **637**, 531; (*d*) A.-R. Ibrahim, X. Li, Y. Zhou, Y. Huang, W. Chen, H. Wang and J. Li, *Int. J. Mol. Sci.*, 2015, **16**, 7960.

71 T. Iwasaki, R. Nakatsuka, K. Murase, H. Takata, H. Nakamura and S. Watano, *Int. J. Mol. Sci.*, 2013, **14**, 9365.

72 (*a*) M. Zarghani and B. Akhlaghinia, *Appl. Organomet. Chem.*, 2015, **29**, 683; (*b*) Z. Zarei and B. Akhlaghinia, *Chem. Pap.*, 2015, **69**, 1421; (*c*) M. Zarghani and B. Akhlaghinia, *RSC Adv.*, 2015, **5**, 87769; (*d*) N. Razavi and B. Akhlaghinia, *RSC Adv.*, 2015, **5**, 12372; (*e*) N. Razavi and B. Akhlaghinia, *New J. Chem.*, 2016, **40**, 447; (*f*) S. S. E. Ghodsinia and B. Akhlaghinia, *RSC Adv.*, 2015, **5**, 49849; (*g*) R. Jahanshahi and B. Akhlaghinia, *RSC Adv.*, 2015, **5**, 104087; (*h*) R. Jahanshahi and B. Akhlaghinia, *RSC Adv.*, 2016, **6**, 29210; (*i*) M. Zarghani and B. Akhlaghinia, *RSC Adv.*, 2016, **6**, 31850; (*j*) M. Zarghani and B. Akhlaghinia, *RSC Adv.*, 2016, **6**, 38592; (*k*) N. Yousefi Siavashi, B. Akhlaghinia and M. Zarghani, *Res. Chem. Intermed.*, 2016, **42**, 5789; (*l*) E. Karimian, B. Akhlaghinia and S. S. E. Ghodsinia, *J. Chem. Sci.*, 2016, **128**, 429; (*m*) M. Zarghani and B. Akhlaghinia, *Bull. Chem. Soc. Jpn.*, 2016, **89**, 1192; (*n*) S. S. E. Ghodsinia, B. Akhlaghinia and R. Jahanshahi, *RSC Adv.*, 2016, **6**, 63613.

73 F. Heidari, M. E. Bahrololoom, D. Vashaee and L. Tayebi, *Ceram. Int.*, 2015, **41**, 3094.

74 M. E. Bahrololoom, M. Javidi, S. Javadpour and J. Ma, *J. Ceram. Process Res.*, 2009, **10**, 129.

75 M. M. A. Nikje, L. Sarchami and L. Rahmani, *Int. J. Biomed. Nanosci. Nanotechnol.*, 2015, **11**, 39.

76 J. Venkatesan and S. K. Kim, *Materials*, 2010, **3**, 4761.

77 L. Xiaoying, F. Yongbin, G. Dachun and C. Wei, *Key Eng. Mater.*, 2007, **342**, 213.

78 Z. Zhang, Z. Yuan, D. Tang, Y. Ren, K. Lv and B. Liu, *ChemSusChem*, 2014, **7**, 3496.

79 P. Li, Z. P. Xu, M. A. Hampton, D. T. Vu, L. Hung and V. Rodolgh, *J. Phys. Chem. C*, 2012, **116**, 10325.

80 M. S. Sajadi, M. Meskinfam and H. Jazdarreh, *Int. J. Nano Dimens.*, 2010, **1**, 57.

81 S. Li, H. Bai, J. Wang, X. Jing, Q. Liu, M. Zhang, R. Chen, L. Liu and C. Jiao, *Chem. Eng. J.*, 2012, **193**, 372.

82 N. Mupparapu, N. Battini, S. Battula, S. Khan, R. A. Vishwakarma and Q. N. Ahmed, *Chem.–Eur. J.*, 2014, **20**, 1.

83 S. K. Movahed, N. F. Lehi and M. Dabiri, *RSC Adv.*, 2014, **4**, 42155.

84 B. J. Borah, S. J. Borah, L. Saikia and D. K. Dutta, *Catal. Sci. Technol.*, 2014, **4**, 1047.

85 H. Sharghi, A. Khoshnood and R. Khalifeh, *Iran. J. Sci. Technol.*, 2012, **36**, 25.

86 J. V. Madhav, B. S. Kuarm, P. Someshwar, B. Rajitha, Y. T. Reddy and P. A. Crooks, *Synth. Commun.*, 2008, **38**, 3215.